IOPscience iopscience.iop.org

Home Search Collections Journals About Contact us My IOPscience

A measuring system for mechanical characterization of thin films based on a compact *in situ* micro-tensile tester and SEM moiré method

This article has been downloaded from IOPscience. Please scroll down to see the full text article.

2013 J. Micromech. Microeng. 23 085021

(http://iopscience.iop.org/0960-1317/23/8/085021)

View the table of contents for this issue, or go to the journal homepage for more

Download details:
IP Address: 159.226.36.113
The article was downloaded on 16/09/2013 at 03:33

Please note that terms and conditions apply.

IOP PUBLISHING JOURNAL OF MICROMECHANICS AND MICROENGINEERING
J. Micromech. Microeng. **23** (2013) 085021 (7pp) doi:10.1088/0960-1317/23/8/085021

A measuring system for mechanical characterization of thin films based on a compact *in situ* micro-tensile tester and SEM moiré method

Yanjie Li[1,2], Minjin Tang[1], Huimin Xie[1,4], Ronghua Zhu[1], Qiang Luo[3] and Changzhi Gu[3]

[1] AML, Department of Engineering Mechanics, Tsinghua University, Beijing, 100084, People's Republic of China
[2] School of Civil Engineering and Architecture, University of Jinan, Jinan, 250022, People's Republic of China
[3] Institute of Physics, Chinese Academy of Sciences, Beijing, 100190, People's Republic of China

E-mail: xiehm@mail.tsinghua.edu.cn

Received 25 March 2013, in final form 7 June 2013
Published 12 July 2013
Online at stacks.iop.org/JMM/23/085021

Abstract
A measuring system for mechanical characterization of thin films based on a compact *in situ* micro-tensile tester and scanning electron microscope (SEM) moiré method is proposed. The load is exerted by the tensile tester and the full field strain is measured by SEM moiré method. The configuration of the tensile tester and the principle of SEM moiré method are introduced. In the tensile tester, a lever structure is designed to amplify the displacement imposed by lead–zirconate–titanate (PZT) actuator. The SEM moiré method is applied to measure the strain of the thin film, including both the average strain in the gage section and the local strain distribution at a specific region. As an application, the measuring system is applied to characterize the mechanical property of the free-standing aluminum thin film. The experimental results demonstrate the feasibility of the system and its good application potential for mechanical behavior analysis of film-like materials.

(Some figures may appear in colour only in the online journal)

1. Introduction

Thin films have been widely applied in micro-electronics and micro-electro-mechanical systems (MEMS) as structural materials, which means the mechanical properties of thin films used will directly influence the performance of micro-electronics and MEMS. Therefore it is necessary to accurately evaluate their mechanical properties, including elastic properties, residual stresses, fracture strength and fatigue lifetimes, to obtain the optimum performances.

The size of thin films is usually of the order of micrometers, much smaller than bulk materials, which imposes a great challenge to their mechanical characterization. However, by the effort of many researchers, several testing methods including nanoindentation, micro-beam bending, bulge testing, micro-tensile testing and resonance have been developed [1]. Among others micro-tensile testing, the standard method for bulk materials, would be the most favorable way to measure tensile and fatigue properties since it generates a uniform state of stress and strain. However, there are two key issues to solve for this method due to the tiny size of thin films: the handling and gripping of the micro-specimen and the strain measurement.

In order to overcome the above mentioned difficulties and realize tension tests of thin films, various measuring systems and techniques have been developed. Tsuchiya *et al* developed a tensile tester using an electrostatic-force grip in a scanning electron microscope (SEM) chamber to evaluate the tensile

[4] Author to whom any correspondence should be addressed.

 © 2013 IOP Publishing Ltd Printed in the UK & the USA

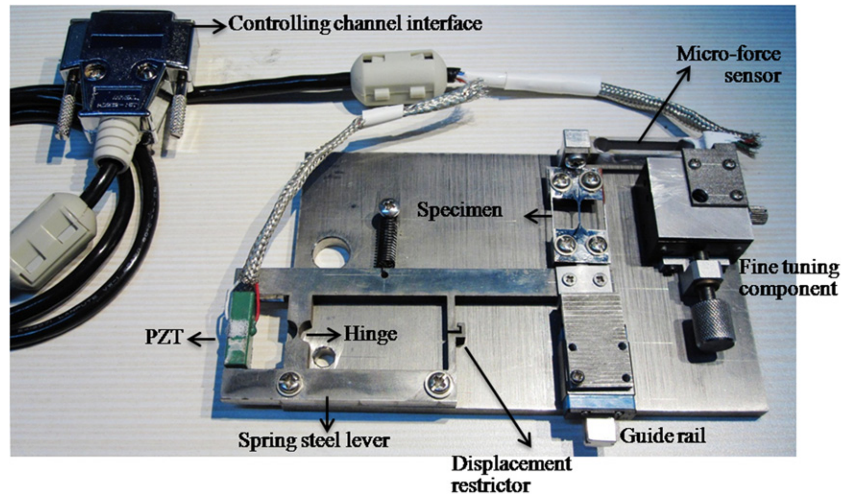

Figure 1. Self-developed micro-tensile testing set-up for low dimensional material under SEM.

strength of thin films [2, 3]. Sharpe *et al* conducted tensile tests of polysilicon by electrostatic gripping and measured the strain through interferometric strain/displacement gage (ISDG) using reflective markers deposited on the specimen [4]. By keeping one end of the specimen fastened to the substrate and the other glued to a silicon carbide fiber attached to a 30 g load cell mounted on a piezoelectric translation stage, Sharpe *et al* stretched 1.0 μm thick silicon dioxide thin film and measured its strain by digital imaging of two gold lines applied to the gage section of the transparent specimen [5]. Haque *et al* designed an on-chip system for *in situ* micro-tensile testing under SEM or transmission electron microscope (TEM) [6]. By measuring the diffraction pattern resulting from the illumination of the grating with monochromatic light, Gaspar *et al* monitored the period variations of integrated 2D reflective grating on silicon nitride (SiNx) thin films to evaluate their strain [7].

In this paper, a measuring system for mechanical characterization of thin films based on a compact *in situ* micro-tensile tensile tester and SEM moiré method is developed. The compact tensile tester is specially designed for *in situ* micro-tensile testing, which is matched with the stage of the SEM. SEM moiré is a high sensitivity full field deformation measurement method [8, 9], which can not only obtain the average strain in the gage section but also the local strain at a specific region like the strain around the defects like crack, hole or interface [10–13].

2. The measuring system

2.1. Tensile tester [14]

In order to realize *in situ* loading under SEM, a micro-tensile tester is developed, which consists of a spring steel lever, a lead–zirconate–titanate (PZT) actuator, a specimen, a fine tuning component, a micro-force sensor, a guide rail and a controlling channel interface, as shown in figure 1. This set-up is an upgraded version of the set-up presented in [15]. When being compared with the previous one, more components have been added, including the micro-force sensor, the guide rail and the controlling channel interface. In addition, this set-up is specially designed to be more compact in consideration of the limited chamber space of the SEM. The details of each component will be introduced as follows.

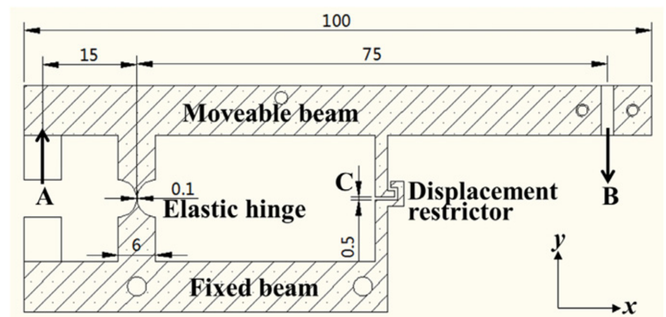

Figure 2. Schematic of spring lever structure.

(1) The spring lever structure
It is the core component of the whole set-up, which is manufactured by precision wire cutting. As shown in figure 2, it consists of an elastic hinge, a fixed beam, a moveable beam and a displacement restrictor. Two semicircles in diameter of 5.9 mm are cut off from the steel beam in width of 6 mm, thus the smallest width of elastic hinge is 0.1 mm. Therefore, spring steel with a high yield strength and good elasticity is used to avoid the failure of the hinge. The fixed beam is attached to the bottom plate through two screw holes and the moveable beam will rotate around the elastic hinge. It should be noted that the distance between point A and the elastic hinge along axis x is 15 mm and the distance between point B and the elastic hinge along axis x is 75 mm. If the displacement is applied on the point A by a PZT actuator, then the point B will move toward the opposite direction and its displacement will be five times of that of point A. The amplification of actuated displacement is realized through the lever structure. The displacement restrictor will restrict the displacement of point C within 0.5 mm so that the rotation of the moveable beam will not be too

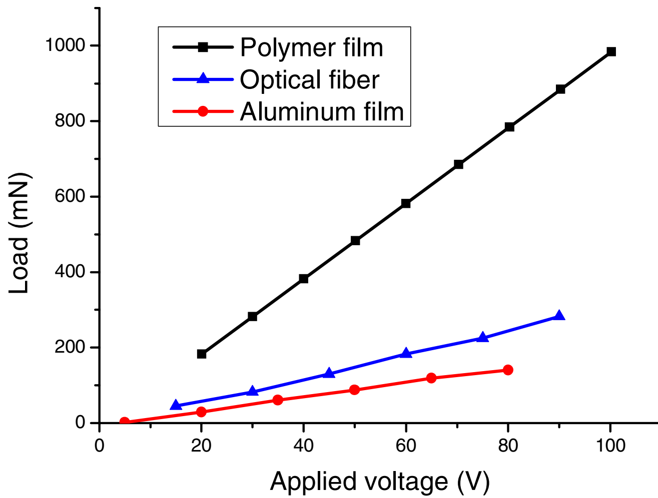

Figure 3. Relation curves between the imposed load and the applied volatge.

large to destroy the lever structure during the assembling and transporting process.

(2) The PZT actuator
It is produced by the NEC Corporation and is 20 mm × 5 mm × 5 mm. The displacement accuracy has reached nanometer scale. The maximum applied voltage and elongation are 150 V and 22 μm respectively. Therefore the maximum elongation of thin film specimen is about 110 μm.

To check out the reliability of the PZT actuator, tensile tests of the polymer thin film, the optical fiber and the aluminum film have been conducted. The relation curves between the load and the applied voltage have been acquired as shown in figure 3. It can be seen that the linearity is pretty good for these three kinds of materials, which verified the reliability of the PZT actuator.

(3) The fine tuning component
The bottom part of the fine tuning component is fixed on the bottom plate and the upper part can be adjusted on micrometer scale along y direction with the maximum displacement of 2 mm. The fine tuning component is to adjust the position of the micro-force sensor and prestretch the specimen.

(4) The specimen
It can be thin film or film-like low dimensional materials.

(5) The micro-force sensor
It is in the form of cantilever beam with measurement range of 1 N and accuracy of 0.5 mN (0.5 ‰). One end is fixed to the upper part of fine tuning component and the other end to the specimen.

(6) The guide rail
The bottom part of guide rail is adhered to the bottom plate and the upper part is attached to the moveable beam. In this way, the rotation of the moveable beam is converted into translation and the out of plane rotation is avoided.

(7) The controlling channel interface
It is connected to the four lines of micro-force sensor, two lines of PZT actuator and ground wire. In this way, the displacement loading is realized by applying the voltage to the PZT actuator and the load is measured by the micro-force sensor and displayed on its controller outside the SEM. All the conductor lines and the joint points have been shielded to reduce their influence to the electron beam of SEM and to ensure the imaging quality.

In summary, this testing set-up is a compact system, which can be matched with the SEM chamber, and thus *in situ* micro-tensile testing and real time observation of thin films can be realized under the SEM.

2.2. SEM moiré method

In SEM moiré method, the horizontal and parallel scanning lines can be regarded as the reference grating. SEM scanning moiré is generated by the superposition of the specimen grating and the reference grating with almost identical frequency.

The frequency of reference grating is expressed as [16, 17]

$$f_r = \frac{MN}{L_0} \tag{1}$$

where M is the magnification of SEM, N is the number of scanning lines and L_0 is the vertical gauge length of SEM monitor, which is a constant.

Since L_0 is a constant, the frequency of the scanning lines is linearly proportional to the magnification for a specified number of scanning lines. In other words, the frequency of reference grating can be adjusted by altering the magnification of SEM. Therefore the relationship between the frequency of reference grating and the magnification is calibrated in advance to get moiré fringes more conveniently. The reference grating pitch, which is equal to the spacing between adjacent pixels, is measured using the scale bar, then the frequency is obtained. This allows us to capture SEM images at different magnifications and measure the scale bar to obtain the corresponding frequencies of the reference grating. The data points can be plotted and the linear fit added to obtain their relation expression. For FEI Siron 400NC used in our experiments, the number of scanning lines is 484, the relation curve between the frequency of reference grating and the magnification is shown in figure 4 and their relation expression is fitted as $M = 0.446f_r$.

When the frequency of the specimen grating is equal to that of the reference grating and their directions are parallel, no fringes will appear. But a small frequency mismatch will lead to moiré fringes. The larger the mismatch is, the denser the fringes are. According to the relation expression between the frequency of reference grating and the magnification, M_0, the magnification at which no fringes are formed, can be derived. It is easy to observe moiré fringes by adjusting the magnification around M_0.

Moiré fringes are a series of isothetic lines of displacement [18], thus the displacement field and the strain field can be obtained by analyzing the fringes. The equations for displacement and direct strain are

$$v = Np_r \tag{2}$$

$$\varepsilon = p_r/d \tag{3}$$

where N is the order of the fringe, p_r is the pitch of the reference grating, there is $p_r = 1/f_r$, and d is the spacing of moiré fringes.

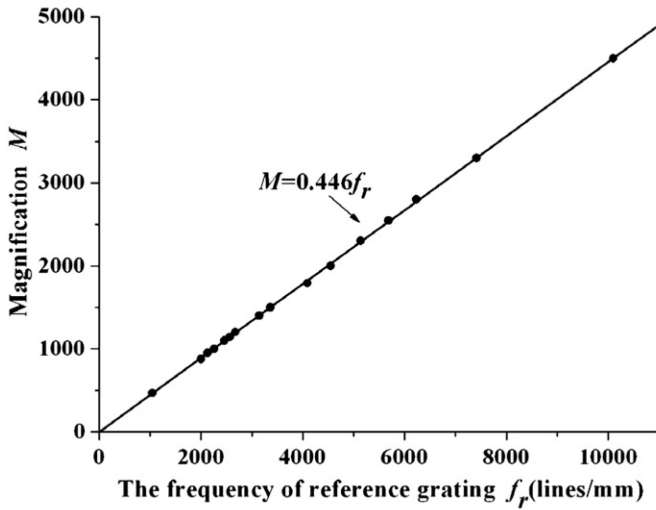

Figure 4. Relation curve between the frequency of reference grating and magnification under FEI Siron 400NC [16].

3. Micro-tensile tests of aluminum film

3.1. Sample preparation

As shown in figure 5, the fabrication of thin aluminum film beam consists of six steps:

(1) Spraying photoresist
UV positive photoresist BP212–7S is sprayed on glass substrate using a self-developed coating device with a rotating speed of 1450 r/m and prebaked at 90 °C for 15 min.
(2) Coating aluminum film
A layer of aluminum film in thickness of about 2 μm is coated on the photoresist by vacuum evaporation.
(3) Spraying photoresist
(4) UV exposure
The duration time of this exposure is 1.5 min
(5) Developing with 1/1000 sodium hydroxide solution
(6) Etching in H_3PO_4.

Finally, the photoresist on the two ends of the beam is removed by exposure and developing and an aluminum film beam is fabricated on glass substrate. It is then adhered to the loading frame [19] with epoxy adhesive and cured for 24 h at room temperature. Then it is immersed in acetone for 2 h to remove the residual photoresist and the glass substrate is taken away gently, and the aluminum film beam is then finally transferred to the aluminum frame successfully, as shown in figure 6. The aluminum frame is about 28 mm × 12 mm with a rectangular window through the center. The frame protects the specimen from damage during handling and allows the specimen to be aligned to the tensile axis before the frame is fixed on the grips of the tensile apparatus. The smooth section of the specimen is approximately 10 mm long by 500 μm wide. The last step in preparing the specimen for testing is the removal of the sides of the aluminum frame, which is chipped out with a sharp tool slowly and carefully.

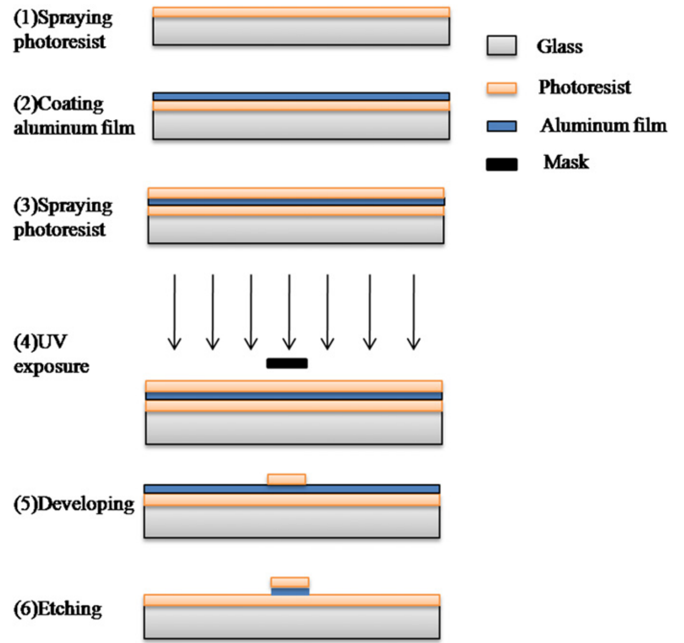

Figure 5. The fabrication steps of thin aluminum film beam on glass substrate.

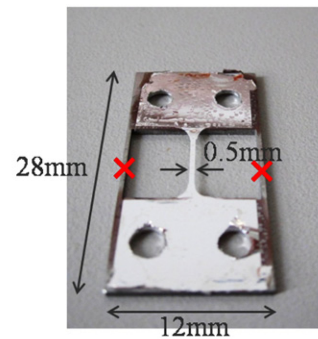

Figure 6. Aluminum film beam transferred on the loading frame, × represents the cutting off position of the frame.

3.2. Grating fabrication

Gratings are the basic deformation carrier for the SEM moiré method. The thickness of aluminum film is in the scale of microns, which means it is small, delicate and difficult to handle. To avoid damaging the thin aluminum film, focused ion beam (FIB) is used to fabricate high frequency grating due to its capability for direct writing on a specific region [20]. FIB is an advanced micro/nano-scale micromachining tool, which possesses two major functions: milling and deposition. Here FIB milling is used to fabricate high frequency grating, which etches off a clean hole from the exposed material surface by accelerating the focused ion beam on a specific site. The grating fabrication consists of grating design and parameters optimization. First, the pattern of specimen grating is designed and input into the FIB system. Then the optimized parameters are obtained through several trial tests and the specimen grating is fabricated under this condition.

The specimen grating is designed to be parallel grating of 1000 lines/mm. FIB milling is conducted under a dual

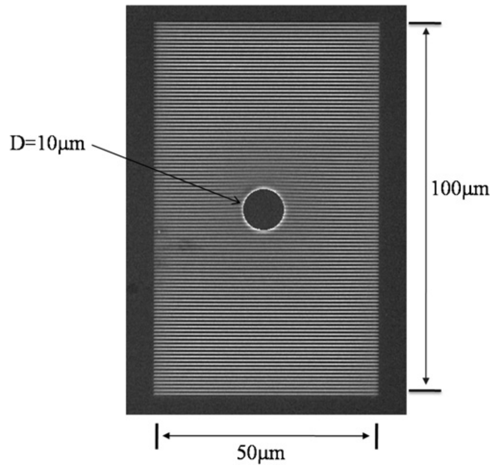

Figure 7. Diagram of fabricated gratings, a hole in diameter of 10 μm is fabricated in the center of the grating region.

beam system, Tescan Lyra 3, which combines FIB and SEM. FIB is for micromachining and SEM is for real time observation. The ion beam current is 127 pA. The grating size is 100 μm × 50 μm, as shown in figure 7, and the setting depth is 0.5 μm. From our experience, the actual milling depth is usually far smaller than the the setting depth [21], about 1/10 of the setting depth or less, which assures that the mechanical property of the aluminum film will not be influenced by the milled micro-trenches. The parallel mode is adopted during the fabrication process. After the fabrication of the grating, a hole 10 μm in diameter is fabricated by FIB milling in order to observe local strain concentration of the aluminum film.

3.3. Experimental procedure

The load frame was placed on the tensile tester of SEM and fixed through four screw holes. The sides of the frame were cut carefully and slowly to ensure the integrity of the micro-specimen. The tensile tester was then put into the chamber of the SEM (FEI siron 400 NC). The conductor lines were then connected to the external power supply through the channel interface. The aluminum film is then stretched by applying voltage to the PZT actuator. The relationship between the applied voltage and the micro-force is obtained by calibration tests. The moiré fringes were recorded before applying the voltage. Then the voltage was increased up to 100 V with a step of 10 V and the moiré fringes were recorded with the micro-force at each step when the voltage was applied for a while and its magnitude was stable. The moiré fringes at 0 V and 100 V are shown in figure 8. It can be seen that in the 100 μm length range, the number of dark moiré fringes changed from 11 to 12. It should be noted that the moiré fringes around the hole were denser than that far away from the hole, which implies that the strain is larger around the hole.

3.4. Results and discussions

The average strain is calculated from the moiré fringes about 7.5 μm, which is one and a half times of the radius of the hole, from the edge of the hole to reduce its influence. The virtual strain method was used here [22]. The virtual strain was calculated according to the moiré fringes before and after deformation. Then the real strain is

$$\varepsilon = \varepsilon_v^d - \varepsilon_v^i \tag{4}$$

where ${\varepsilon_v}^i$ and ${\varepsilon_v}^d$ are virtual strain before and after deformation, which can be calculated through equation (3).

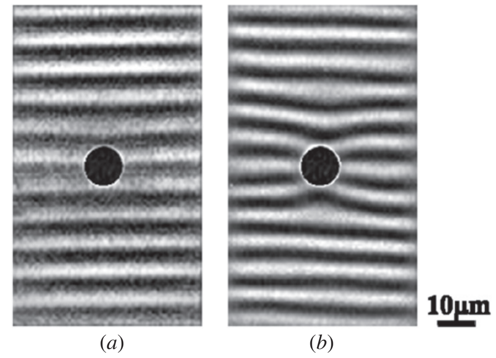

Figure 8. Moiré fringes at different voltages (*a*) 0 V; (*b*) 100 V.

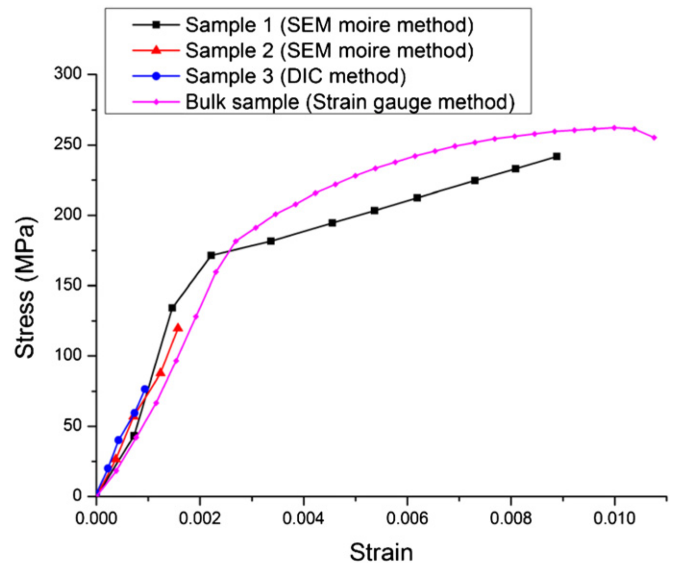

Figure 9. Stress–strain curve.

The stress can be obtained by dividing the cross section area of thin film from the recorded load. Then the stress–strain curve was plotted as sample 1 in figure 9. It can be seen that the thin film begins to yield from about 175 MPa. The first three groups of stress–strain data are used to linearly fit to obtain Young's modulus, which is 80.2 GPa. To test the reliability and repeatability of the measuring system, another sample was tested (see sample 2 in figure 9) but only elastic part is illustrated and the Young's modulus is calculated as 74.5 GPa. In comparison, a thin film sample measured with digital image correlation (DIC) method and bulk sample measured with strain gauge method are also displayed in figure 9. Their Young's moduli are 78.6 GPa and 70.2 GPa respectively. The results for thin films are in the same range and their relative error is within 10%. The error sources of the measurement fall into two categories: the

stress measurement and the strain measurement. The former depends on the load and the size of the cross section of specimen. The load was obtained through the micro-force sensor with the measurement range of 1 N and accuracy of 0.5 mN (0.5 ‰). The width and the thickness of thin films were measured through microscope observation, which introduced some artificial errors and these errors are reduced through calculating the mean value of several measurements. The strain was calculated by analyzing the moiré fringes with fringe centering technique [23], whose accuracy strongly depends on the quality of moiré fringes. Since the quality of gratings directly influence the quality of moiré fringes, high quality gratings are necessary. In our experiments, several trial tests were conducted to obtain the optimum parameters of FIB systems before grating fabrication. It can also be seen that the Young's modulus of thin film samples is larger than that of bulk materials. The reason is that the size (especially the thickness) of thin film is in the micrometer scale, much smaller than the bulk sample, which is on the millimeter scale. It is not difficult to understand this phenomenon, since the defects are decreasing with the decrease of specimen size and the resistance ability to deformation is enhanced.

In order to study the effect of strain concentration of the hole at micro-scale, the tensile strain around the hole when the voltage is 100 V was calculated as 8.8% and the average strain was 3.1%. Therefore, the strain around the hole is about 3.5 times of the average strain. According to the theory of elastic mechanics, the strain concentration of a hole in an infinite plate is 3 for bulk material. In our case, the specimen width is 500 μm and the diameter of the hole is 10 μm, which can be regarded as an infinite plate. In our opinion, the larger result is probably caused by the plastic strain and the dimension effect.

4. Conclusions

A measuring system for mechanical characterization of thin films based on self-developed tensile tester and SEM moiré method is proposed. The tensile tester is to exert load to thin films and SEM moiré is to measure the strain. The tensile tester adopts displacement loading through high precision PZT actuator. A lever structure is designed to amplify the actuation displacement for five times. The maximum elongation of specimen is about 110 μm and the maximum tensile load is 1 N. The SEM moiré method can not only obtain the average strain of thin films but also the local strain distribution.

The measuring system is applied to the mechanical characterization of the free-standing aluminum thin film. To fabricate the deformation carrier of the SEM moiré method on the specimen surface, FIB milling is used and gratings of 1000 lines/mm are fabricated. The stress–strain curve is obtained and the Young's modulus is derived. The strain concentration around a hole is also quantitatively analyzed. The experimental results demonstrate the feasibility and reliability of the proposed measuring system and its application potential for mechanical characterization of thin film-like materials.

Acknowledgments

The authors are grateful to the financial support from the National Basic Research Program of China ('973' Project) (grant no 2010CB631005, 2011CB606105), the National Natural Science Foundation of China (grant no 11232008, 91216301, 11227801, 11172151), Tsinghua University Initiative Scientific Research Program, the initiative Scientific Research Program and the Doctoral Program of University of Jinan (grant no XBS1307).

References

[1] Stanimirović Z and Stanimirović I 2009 *Mechanical Properties of MEMS Materials, a chapter of Micro Electronic and Mechanical Systems* ed K Takahata (Croatia: Intech)

[2] Tsuchiya T, Tabata O, Sakata J and Taga Y 1998 Specimen size effect on tensile strength of surface-micromachined polycrystalline silicon thin films *J. Microelectromech. Syst.* **7** 106–13

[3] Tsuchiya T, Inoue A and Sakata J 2000 Tensile testing of insulating thin films; humidity effect on tensile strength of SiO2 films *Sensors Actuators* A **82** 286–90

[4] Sharpe W, Turner K and Edwards R 1999 Tensile testing of polysilicon *Exp. Mech.* **39** 162–70

[5] Sharpe W, Pulskamp J, Gianola D, Eberl C, Polcawich R and Thompson R 2007 Strain measurements of silicon dioxide microspecimens by digital imaging processing *Exp. Mech.* **47** 649–58

[6] Haque M and Saif M 2002 *In-situ* tensile testing of nano-scale specimens in SEM and TEM *Exp. Mech.* **42** 123–8

[7] Gaspar J, Nurcahyo Y, Ruther P and Paul O 2007 Mechanical characterization of silicon nitride thin-films using microtensile specimens with integrated 2D diffraction gratings *IEEE 20th Int. Conf. Micro Electro Mechanical Systems* pp 223–6

[8] Xie H M, Shang H X, Dai F L, Li B and Xing Y M 2004 Phase shifting SEM moire method *Opt. Laser Technol.* **36** 291–7

[9] Kishimoto S 2012 Electron Moiré method *Theor. Appl. Mech. Lett.* **2** 011001

[10] Kishimoto S, Tanaka Y, Yin F, Kagawa Y and Nagai K 2011 Strain distribution measurement in laminated martensitic/austenitic steel during a compressive test by the electron moire method *J. Strain Anal. Eng. Des.* **46** 1–6

[11] Kishimoto S, Huimin X and Shinya N 2000 Electron moire method and its application to micro-deformation measurement *Opt. Laser Eng.* **34** 1–14

[12] Lee O and Read D 1995 Micro-strain distribution around a crack tip by electron beam moire methods *J. Mech. Sci. Technol.* **9** 298–311

[13] Du H, Xie H, Guo Z, Pan B, Luo Q, Gu C, Jiang H and Rong L 2007 Large-deformation analysis in microscopic area using micro-moire methods with a focused ion beam milling grating *Opt. Laser Eng.* **45** 1157–69

[14] Tang M 2012 The study of moiré grating fabrication method by nanoimprint lithography and the characterization of grating structures *PhD Thesis* Department of engineering mechanics, Tsinghua University pp 61–5

[15] Hua T, Xie H M, Feng X, Wang X, Zhang J M, Chen P W and Zhang Q M 2009 A new dynamic device for low-dimensional materials testing *Rev. Sci.Instrum.* **80** 12608

[16] Li Y, Xie H, Tang M, Zhu J, Luo Q and Gu C 2012 The study on microscopic mechanical property of polycrystalline with SEM moiré method *Opt. Laser Eng.* **50** 1757–64

[17] Read D and Daily J 1996 Theory of electron beam moire *J. Res. Natl Inst. Stand. Technol.* **101** 47–62
[18] Durelli A and Parks V 1970 *Moire Analysis of Strain* (Englewood Cliffs, NJ: Prentice-Hall)
[19] Seguineau C, Ignat M, Malhaire C, Brida S, Lafontan X, Desmarres J M, Josserond C and Debove L 2008 Micro-tensile tests on micromachined metal on polymer specimens: elasticity, plasticity and rupture *Symp. Design, Test, Integration and Packaging of MEMS/MOEMS* pp 8–10
[20] Tseng A A 2005 Recent developments in nanofabrication using focused ion beams *Small* **1** 924–39
[21] Li Y, Xie H, Guo B, Luo Q, Gu C and Xu M 2010 Fabrication of high-frequency moiré gratings for microscopic deformation measurement using focused ion beam milling *J. Micromech. Microeng.* **20** 055037
[22] Kishimoto S, Shinya N and Mathew M 1997 Application of electron beam lithography to study microcreep deformation and grain boundary sliding *J. Mater. Sci.* **32** 3411–7
[23] Wang Z Y 2003 Development and application of computer-aided fringe analysis *PhD Thesis* Department of Mechanical Engineering, University of Maryland pp 53–66